Atmospheric Environment
Manuscript Draft

Manuscript Number: ATMENV-D-17-00208

Title: Isotopic variability of copper, zinc and lead in atmospheric particulate matter and related sources in London and implications for source tracing

Article Type: Research Paper

Keywords: atmospheric particulate matter, sources, isotopes

Abstract: This study investigates the potential of stable isotope ratios to trace metals in particulate matter (PM) of a megacity. To this end, the temporal isotope variability of Cu, Zn and Pb were determined during two weeks in PM10 collected in London at road sites with different traffic densities and in local sources, including non-combustion traffic emissions (tires and brakes), road furniture (road paint, manhole cover and road tarmac surface) and road dust. Iron, Ba and Sb were used as proxies for emissions derived from brake pads, and Cr, Ni, and V for emissions from fuel oil and other high temperature industrial processes. The isotopic composition of Pb (expressed using 206Pb/207Pb) ranges between 1.1137 and 1.1364. The isotope ratios of Cu and Zn expressed as □65CuNIST976 and □66ZnLyon range between -0.01 and +0.51 ‰ and between -0.21 and +0.33 ‰, respectively. No significant differences in the isotope signatures of these three metals between the two sites were found, suggesting similar sources at both sites. The stable isotope composition of Pb suggests that re-suspended road dust, which contains re-mobilized Pb from past use of leaded gasoline and other sources such as tires, brakes, manhole cover, road paint or road surface, dominate. The Cu and Zn isotope signatures of tires, brakes and road dust overlap with the signatures of PM10. The correlation between the enrichment of Sb and other tracers of brakes such as Cu, Fe and Ba in PM10 support the previously established hypothesis that Cu is predominantly derived from non-exhaust traffic emissions in urban environments (Ochoa Gonzalez et al., 2016). The relationship between the Cu/Sb ratios and the Cu isotope composition demonstrates that samples of PM10 with low Cu/Sb ratios between 5.8 and 11.6, which fall within the range of Cu/Sb previously found for brakes, show lighter copper isotopic signatures with □65CuNBS976 ranging between -0.01 and +0.51‰ and these isotope signatures largely overlap with the Cu isotope signatures in brakes (□65CuNIST976 = +0.28±0.10‰ - +0.63±0.14‰). The Zn signatures in PM10 at the two study sites overlap with the signatures of tires and brakes. However, additional sources, such as those from high temperature industrial emissions that impart isotopically light Zn, need to be invoked to explain the light signatures found in 3 out of 18 samples. This hypothesis is supported by the enrichment of V and Ni in the PM10.

*Manuscript
Click here to download Manuscript: Manuscript.pdf Click here to view linked References

Isotopic variability of copper, zinc and lead in atmospheric particulate matter and related sources in London and implications for source tracing

Shuofei Dong[1,2], Raquel Ochoa Gonzalez[1*], Roy M. Harrison[3,4], David Green[5], Robin North[6], Geoff Fowler[1] and Dominik Weiss[1]

[1]Imperial College London, Department of Earth Science and Engineering, London, SW7 2AZ, UK
[2]CRPG, UMR 7358 CNRS-UL, Nancy 54500, France
[3]National Centre for Atmospheric Sciences, Division of Environmental Health and Risk Management, University of Birmingham, B15 2TT, UK
[4]Department of Environmental Sciences / Center of Excellence in Environmental Studies, King Abdulaziz University, PO Box 80203, Jeddah, 21589, Saudi Arabia
[5]Centre for Environment and Health, King's College London, London SE1 9NH, UK
[6]Transport Systems Catapult, Milton Keynes, MK9 1BP, UK

*Corresponding author
E-mail: raquelocglez@yahoo.es
Tel: +44 (0)20 7594 63 83

Abstract

This study investigates the potential of stable isotope ratios of trace metals in particulate matter (PM) of a megacity. To this end, the temporal isotope variability of Cu, Zn and Pb were determined during two weeks in PM_{10} collected in London at road sites with different traffic densities and in local sources, including non-combustion traffic emissions (tires and brakes), road furniture (road paint, manhole cover and road tarmac surface) and road dust. Iron, Ba and Sb were used as proxies for emissions derived from brake pads, and Cr, Ni, and V for emissions from fuel oil and other high temperature industrial processes.

The isotopic composition of Pb (expressed using $^{206}Pb/^{207}Pb$) ranges between 1.1137 and 1.1364. The isotope ratios of Cu and Zn expressed as $\delta^{65}Cu_{NIST976}$ and $\delta^{66}Zn_{Lyon}$ range between -0.01 and +0.51 ‰ and between -0.21 and +0.33 ‰, respectively. No significant differences in the isotope signatures of these three metals between the two sites were found, suggesting similar sources at both sites. The stable isotope composition of Pb suggests that re-suspended road dust, which contains re-mobilized Pb from past use of leaded gasoline and other sources such as tires, brakes, manhole cover, road paint or road surface, dominate. The Cu and Zn isotope signatures of tires, brakes and road dust overlap with the signatures of PM. The correlation between the enrichment of Sb and other tracers of brakes such as Cu, Fe and Ba in PM_{10} support the previously established hypothesis that Cu is predominantly derived from non-exhaust traffic emissions in urban environments (Ochoa Gonzalez et al., 2016). The relationship between the Cu/Sb ratios and the Cu isotope composition demonstrates that samples of PM_{10} with low Cu/Sb ratios between 5.8 and 11.6, which fall within the range of Cu/Sb previously found for brakes, show lighter copper isotopic signatures with $\delta^{65}Cu_{NBS976}$ ranging between -0.01 and +0.51 ‰ and these isotope signatures largely overlap with the Cu isotope signatures in brakes ($\delta^{65}Cu_{NIST976}$ = +0.28±0.10 ‰ - +0.63±0.14 ‰). The Zn signatures in PM_{10} at the two study sites overlap with the signatures of tires and brakes. However, additional sources, such as those from high temperature industrial emissions that impart isotopically light Zn, need to be invoked to explain the light signatures found in 3 out of 18 samples. This hypothesis is supported by the enrichment of V and Ni in the PM_{10}.

1. Introduction

Metals in atmospheric particulate matter (PM) are a serious concern as they induce adverse health effects. Cardiopulmonary diseases have been attributed to the capacity of inhaled particles and metals to cause inflammation and injury at the air-lung interface (Costa and Dreher, 1997; Chen and Lippmann, 2009; Gamble and Lewis, 1996; Jarup, 2003; Ozkaynak et al., 1996). Lead exposure damages the human central nervous system and kidneys, affects biochemical processes and impairs psychological and neurobehavioral functions (Tong et al., 2000). Zinc is associated with oxidative stress, which is a contributing factor in many chronic diseases (Prasad et al., 2004; Walsh et al., 1994) and Cu causes damage to proteins and lipids (Brewer, 2010). Thus, developing a full understanding of the major sources of metals in urban PM is critical to control toxic emissions in urban environments.

Previous studies analyzed the sources of multiple elements in urban PM (PM_{10}/$PM_{2.5}$) by using conventional chemical techniques and receptor modeling methods such as chemical mass balances (CMB) and positive matrix factorization (PMF). These suggested that industrial emissions, traffic and dust re-suspension are the major processes that contribute to the metal aerosol burden (Cooper and Watson, 1980; Harrison et al., 1997; Laden et al., 2000; Lin et al., 2010; Manoli et al., 2002; Polissar et al., 2001; Querol et al., 2001; Schauer et al., 1996; Thurston and Spengler, 1985). It is has been suggested that Fe and Cr are associated with the bulk matrix from road dust, Zn from tire wear and brake wear-off and dust re-suspension, Pb from vehicular combustion, Fe from brake drum abrasion, wear-off of engines, tires and brakes (Garg et al., 2000), and V and Ni with emissions from oil combustion (Hjortenkrans et al., 2007; Manoli et al., 2002 Thorpe et al., 2007; Thurston et al., 2011). Copper, Sb and Ba are also abundant in brake lining materials whereas brakes (Garg et al., 2000), yellow road paint and road pavement are typically sources of Cr (Adachi and Tainosho, 2004; Hjortenkrans et al., 2007a; Iijima et al., 2007; Rodriguez et al., 2004; Salma and Maenhaut, 2006; Thorpe and Harrison, 2008).

The success of using metal concentrations in combination with PCA and PMF only to identify single sources for trace metals is limited. PCA does not provide a unique solution because of its simplified approach and the results of PMF vary depending on different uncertainty structures (Samek et al., 2016). Consequently, the use of isotope ratios has been investigated to assist source tracing. This approach was successful for Pb, where isotopes identified leaded gasoline as the main source in urban PM in London, and despite the restrictions in the use of leaded gasoline in the 1980s, a contribution of 60% was still found in west London between 1995 and 1996 (Monna et al., 1997; Noble et al., 2008). Stable isotope systems have been tested for source apportionment of trace elements in PM such as Fe, Sr, Zn and Nd (Flament et al., 2008; Geagea et al., 2008; Majestic et al., 2009; Widory et al., 2010). Zinc isotopes in urban PM were studied in Metz, France (Cloquet et al., 2006), São Paulo, Brazil (Gioia et al., 2008), and Barcelona and London (Ochoa Gonzalez et al., 2016). In Metz, the $\delta^{66}Zn_{Lyon}$ in ambient PM collected in a bus and an urban waste incinerator showed similar values close to +0.12 ‰. In São Paolo, in contrast, Gioia et al. (2008) found lighter ratios and significantly larger variations in $\delta^{66}Zn_{Lyon}$, ranging between -1.05 and -0.46 ‰ in $PM_{2.5-10}$ and between -1.13 and -0.07 ‰ in $PM_{2.5}$. In line with these findings, Ochoa Gonzalez et al. found isotopically light Zn in PM_{10} collected in Barcelona, with $\delta^{66}Zn_{Lyon}$ ranging between -0.45 and -0.83 ‰, and isotopically heavy Cu in coarse PM collected in London during late autumn and the winter season ($\delta^{65}Cu_{NIST976}$= +0.66 - +0.97 ‰) (Ochoa

Gonzalez et al., 2016). The observed light and heavy isotopic signature[s] [o]f the PM were tentatively interpreted as Zn and Cu derived from combustion and smelting processes. Other studies are in line with this interpretation as they showed that residues and flue gas particles from metal refining and coal combustion are highly fractionated relative to the starting materials, with light Zn in the emitted PM (between -0.73 and -0.63 ‰) and heavy Zn in the residues (up to +1.49 ‰) (Mattielli et al., 2009; Ochoa González and Weiss, 2015; Sivry et al., 2008). These signatures seem to partially overlap with the isotope ratios of Zn in anthropogenic materials produced during low temperature processes like galvanisation which show $\delta^{66}Zn_{Lyon}$ between +0.12 and +0.58 ‰ (John et al., 2007). In summary, these studies demonstrated that Cu and Zn isotopes can be used to identify emissions from metal refining and combustion due to their large fractionation, as well as Pb isotopes to assess the contribution from combustion of gasoline.

The aim of this work was to critically test the previous findin[gs] [a]nd to characterize the short-term temporal isotope variability of Cu, Zn and Pb isotopes as a function of the density of traffic in atmospheric PM, as well as the isotopic fingerprints in the sources. To this end, we collected PM_{10} samples at a high and a low traffic density site over a 20-day sampling period during summer in London, UK. Also, potential sources including road furniture (manhole cover, road paint and road tarmac surface), non-combustion vehicle sources (tire and brake wear) and road dust (that represents other potential sources deposited in the road environment) were isotopically characterized. The concentrations of trace elements including Fe, Sb, Ba, Cr, Ni, and V, and enrichment factors (EFs) were combined with the isotope ratios and EFs of Zn, Cu and Pb to assess the contribution of the sources.

2. Materials and methods

2.1. Sample collection

Samples of PM_{10} were collected during 48 h using a Partisol-Plus Model 2025 Sequential Air Sampler (Thermo Scientific, MA, USA) [at] two different road sites in central London between 8th July 2010 and 28th July 2010. Samples were collected at the heavily traffic street canyon Marylebone Road (MR) in London, with more than 80,000 vehicles per day and frequently congested (Charron and Harrison, 2005). The other sampling location (North Kensington, denoted as NK) is a lightly trafficked open urban site situated next to a school playground (Bigi and Harrison, 2010). The sampling site NK has an average daily traffic flow of 8,000 vehicles and the nearest road is more than 30 m away (Abdalmogith and Harrison, 2006). Polytetrafluoroethylene (PTFE) filters were used for PM_{10} collection and leached prior use for 2 days [in] 5 M distilled H[NO3] at 100˚C on a hotplate.

Three samples of road dust were taken from the road side[walk] [e]ach site, one next to the PM sampling tube and two in the two opposite directions from each of the sampling sites. Road furniture (manhole cover and road paint, 2 samples at each site; road tarmac surface, 2 samples at the NK site) were sampled within approximately 10 m of each aerosol sampling site and were stored in plastic bags.

Non-combustion vehicle sources, i.e., tear-off from tires and brakes, were characteri[zed] [u]sing a collection of used tires and new brake pads. Twelve individual tires from various manufacture[rs] [w]ere shredded and mixed before analysis. The brake samples were scratched from the surface of two different brands of brake pads (namely FSB and HBP). All tires and brakes were common commercial brands.

The standard reference material BCR-723 (road dust) and single element solutions (Romil Cu, Romil Zn and NIST-SRM 981 Pb) were used to determine the precision and accuracy of the concentrations and isotope

ratio measurements.

2.2. Sample preparation

The filters were weighted before and after the collection to determine the mass of material, and the metals were leached from the filter with 5 ml of aqua regia for 24 hours followed by 10 ml of 0.5 M HNO_3 for 48 hours on a hotplate at 80˚C. An ultrasonic bath was used for 1 hour every 12 hours to improve the removal efficiency. The filters were then washed with 5 ml 0.5 M HNO_3 three times. The two solutions were mixed and evaporated to dryness before further treatment. The standard BCR-723 (road dust) and all the samples were digested using a c.a. HNO_3: $HClO_4$ mixture (1: sealed PFA vials (Savillex, MN, USA) at 150˚C in a hotplate for 24 hours. The samples were dried and further digested using a mixture of c.a. HNO_3 and HF (1:4) on a hotplate at 140˚C for another 24 hours. The solutions were taken to dryness again. The samples were re-fluxed in 300 µl of c.a. HNO_3 twice. After re-dissolution in 2.5 ml of 0.5 M HNO_3, 0.5 ml was used for concentration measurement using quadrupole ICP-MS and the remaining volume of each solution was prepared for anion exchange column separation of Pb, Cu and Zn.

All the experimental work was carried out in a Class 1000 clean lab and under Class 10 laminar flow hoods at the MAGIC laboratories at Imperial College London. Sub-distilled mineral acids (HNO_3 15 mol l^{-1}, HCl 6 mol l^{-1}), commercial HF (40 % v/v Suprapur, Merck, Germany) and $HClO_4$ (70 % v/v Suprapur, Merck, Germany), and 18.2 MΩ·cm grade Millipore water (Bedford, MA, USA) were used throughout this study.

2.3. Concentration analysis and enrichment factors

The concentration of Fe, Al, Cu, Zn, Sb, Ba, Pb, Cr, Ni and V were determined using quadrupole ICP-MS (Varian, CA, USA). Table S1 shows the concentrations of Cu, Zn, Sb, Ba and Pb for BCR-723 (road dust). The analytical precision is below 6% (n=5, 2SD) and the uncertainty, relative to the indicative values provided by the European Commission Joint Research Centre Institute for Reference Materials and Measurements, is below 11% respect to the reference values for all the elements.

The EFs of the PM_{10} were calculated to assist the source assessment study using Al as as a proxy for the upper continental crust according to Eq. 1,

$$EF_C = \frac{C_{sample}/Al_{sample}}{C_{crust}/Al_{crust}} \quad \text{[Eq. 1]}$$

where C is the element of interest and C_{sample}, Al_{sample}, C_{crust} and Al_{crust} are the concentrations of C and Al in the sample and the continental crust. The average chemical composition of the upper continental crust was used as previously reported (Wedepohl, 1995).

2.4. Isotope ratio analysis of Cu, Zn and Pb

Zinc, Cu and Pb in all of the samples were separated from other matrix elements using methods based on ion exchange chromatography. The details of the Cu, Zn and Pb separation methods and sample treatment are described elsewhere (Dong et al., 2013; Weiss et al., 2004) and summarized in the Supplementary material.

The total procedural blank was < 4 ng for Cu and Zn and < 80 pg for Pb. This contribution was less than 0.01% of the total element content in all samples analyzed and had no significant effect on the accuracy of the

isotope ratio measurements. The details of Zn, Cu and Pb isotope ratio measurements and mass bias correction methods are described elsewhere (Dong et al., 2013; Weiss et al., 2004).

The Romil Cu and Romil Zn solutions were processed and measured with the samples during this study and showed values of $\delta^{65}Cu_{NIST976}$ = +0.17 ± 0.10 ‰ (2SD, n=24) and $\delta^{66}Zn_{Lyon}$ = -9.12 ± 0.08 ‰ (2SD, n=20), respectively. These are within error relative to previous published values for Romil Cu ($\delta^{65}Cu_{NIST976}$ = +0.18 ± 0.06 ‰, n=19, Moeller et al., 2012; $\delta^{65}Cu_{NIST976}$ = +0.18 ± 0.05 ‰, n=4, Ochoa Gonzalez et al., 2016) and Romil Zn ($\delta^{66}Zn_{Lyon}$ = -9.14 ± 0.08 ‰, n=21, Chapman et al., 2006). During this study $^{206}Pb/^{204}Pb$, $^{207}Pb/^{204}Pb$ and $^{208}Pb/^{204}Pb$ for NIST-SRM 981 Pb were 16.9372 ± 0.0021, 15.4954 ± 0.0021 and 36.7158 ± 0.0057 (n=50), respectively which are in good agreement with previous published data (Weiss et al., 2004).

3. Results and discussion

3.1. Source assessment based on concentrations and enrichment factors

The concentrations of PM_{10} and Fe, Cu, Al, Zn, Sb, Ba, Fe, Cr, Pb, Ni and V in the PM_{10} and local sources are shown in Table 1 and Table 2. The concentrations of PM_{10} are approximately twice as high at the MR site (31±7 μg m^{-3}) compared to the NK site (14±3 μg m^{-3}). According to London Air, average hourly concentrations of PM_{10} at the MR and NK sites over the sampling period during July 2010 are 40±15 μg m^{-3} and 16±7 μg m^{-3}, respectively (London Air Website, www.londonair.org.uk).

The concentrations and the EFs of Fe, Cu, Zn, Sb, Ba and Cr in the PM_{10} collected at MR site are much higher than those at NK site (Tables 1 and 3). These elements are highly enriched relative to the natural dust which is represented by the upper continental crust (Table 3), suggesting that they are derived from traffic related emissions. The contents of Sb, Cu, Ba, Zn, and Fe are significant in tires and brakes (McKenzie et al., 2009). The correlations between the EF_{Sb} and those of Cu, Ba, Zn and Fe (Figure 1), show R^2 between 0.8686 and 0.9972, supporting the hypothesis of similar sources in PM at NK and MR, and non-combustion traffic emissions as the main source. The EF_{Sb} and those of typical tracers of brakes (i.e., Cu, Fe and Ba) show similar and very high R^2 (R^2=0.9949-0.9972), suggesting that non-exhaust emissions are the dominant source for these elements in urban PM_{10} in London.

Re-suspension of small particles of road dust may have a significant effect on the generation of PM enriched in metals (Chen et al., 2012). The road dust samples collected at the MR site (MRRD-1, MRRD-2 and MRRD-3) are enriched in Fe, Cu, Zn, Sb, Ba, Cr and Pb compared to road dust at the NK site (NKRD-1, NKRD-2 and NKRD-3) (Table 3), most probably reflecting the higher traffic density. This observation shows the potential of re-suspended road dust being an important source of these elements in urban PM.

Brake wear is the dominant source of Ba in urban and natural PM (Gietl and Klemm, 2009; Gietl et al., 2010; Iijima et al., 2007; Moreno et al., 2015). We find high concentrations of Ba in brakes (311-1288 μg g^{-1}) and samples of manhole cover (115-1055 μg g^{-1}) (Table 2). The concentrations of Ba in the PM_{10} at the NK site (1.6±0.4 ng m^{-3}) are much lower than at the MR site (5.7-83.6 ng m^{-3}), supporting the dominant contribution of brake wear. The concentration of Zn in PM_{10} ranges between 1.4 and 3.1 ng m^{-3} at the NK site and between 3.7 and 40.6 ng m^{-3} at the MR site. The concentration of Cu in PM_{10} ranges between 1.9 and 3.6 ng m^{-3} at the NK site and between 9.4 and 126.4 ng m^{-3} at the MR site. The element concentrations show that the content of Zn in tires and that of Cu in brakes, tires and samples of manhole cover are significantly higher than in other sources (Table 2). In addition, samples of road tarmac surface and manhole cover contain significant amounts

of Zn. Cu/Sb ratios between 3.3 and 9.1 have been used to identify brake wear in PM collected in Cologne, London, Stockholm and Budapest (Hjortenkrans et al., 2007b; Salma and Maenhaut, 2006; Weckwerth, 2001). In this study similar Cu/Sb ratios are observed in PM_{10} with a smaller range between 5.8 and 8.3 (Table 1). The average Cu/Sb ratios in the PM_{10} at the NK site are slightly higher than those in the PM_{10} at the MR site. However, the Cu/Sb ratios in the studied brake pads range between 27.3 and 39.3 and are very large compared with typical values for brakes in PM (Table 2). This observation agrees with the recent restrictions on the use of Sb_2S_3 during the manufacturing process of brake pads due to its potential carcinogenic properties (Hüner et al., 2001).

The concentrations of Cr in the PM_{10} collected at the MR site (0.9-8.2 ng m^{-3}) are higher than those at the NK site (0.3±0.1 ng m^{-3}). Multiple sources including brakes, manhole cover, an old yellow road paint (NKRP-2) and road dust are enriched in this element relative to natural sources (Table 3). However, the positive correlation between the EF_{Sb} and the EF_{Cr} ($R^2 = 0.9385$) in PM_{10} (Figure 1), and between the EF_{Sb} and those of other elements linked with non-exhaust emissions, i.e., Cu and Fe, suggests that not only Fe, but also Cr is mainly controlled by non-exhaust emissions in the urban atmosphere. The concentrations of Fe and EF_{Fe} in the PM_{10} collected at MR are higher than those in the PM_{10} at NK and significantly large concentrations of this element are found in samples of brakes and manhole cover. In addition to these sources, brake discs have been found to contribute significantly to the emissions of PM_{10} enriched in Fe (Wåhlin et al., 2006). The elemental concentrations and EFs of Ni and V are similar in the PM_{10} at both sites, which suggests that these elements are not directly affected by the density of traffic (Tables 1 and 3). Previous studies suggested that Ni and V are derived from fuel oil, gas refineries, and industrial processes (Moreno et al., 2010; Nriagu and Pacyna, 1988; Peltier and Lippmann, 2010), and less significantly from non-exhaust traffic sources (Thorpe and Harrison, 2008). In a recent receptor modelling study conducted using PM_{10} samples collected at the NK site (Beddows et al., 2015)., Ni and V were found to be associated with high concentrations of sulphate in a fuel oil-related factor. Lead concentrations in PM_{10} are slightly higher at the MR site (1.1-8.8 ng m^{-3}) compared to the NK site (1.0±0.3 ng m^{-3}) but the EF_{Pb} are similar at both sites. Some studies based on emissions of metals in PM_{10} and $PM_{2.5}$ suggested that following the phasing out of leaded gasoline, Pb is emitted into the urban atmosphere from fuel and motor oil combustion or brake wear (Lough et al., 2005). The concentrations of Pb in manhole cover, tires and brakes are significant, ranging between 4.0 and 37.9 μg g^{-1} in tires and brakes, and between 56.4 and 693.0 μg g^{-1} in samples of manhole cover (Table 2).

3.2 Source identification of lead using stable isotope ratios

The $^{206}Pb/^{204}Pb$, $^{206}Pb/^{207}Pb$ and $^{208}Pb/^{206}Pb$ isotope ratios determined in the PM_{10} and the sources are shown in Table 4. Figure 2a shows that the Pb isotope ratios in PM_{10} are similar at the MR and NK sites. This observation, and the slightly higher concentrations of Pb in the PM_{10} at the MR site when compared with the NK site (Table 1), suggest that the source(s) at NK and MR sites are the same and there is a direct influence of traffic density on Pb concentrations in PM_{10}. The Pb isotope ratios measured in the PM_{10} in NK ($^{206}Pb/^{204}Pb$ = 17.446-17.598, $^{206}Pb/^{207}Pb$ = 1.1218-1.1304, $^{208}Pb/^{206}Pb$ = 2.1288-1.1382) fall within the respective ranges in MR ($^{206}Pb/^{204}Pb$ = 17.305-17.701, $^{206}Pb/^{207}Pb$ = 1.1137-1.1364, $^{208}Pb/^{206}Pb$ = 2.1246-1.1476). These Pb signatures are significantly different from those of natural sources in the UK ($^{206}Pb/^{207}Pb$= 1.18-1.19) (Monna et al., 1997), which suggests an ongoing contribution of anthropogenic sources in atmospheric PM. The

$^{208}Pb/^{206}Pb$ and $^{206}Pb/^{207}Pb$ isotope ratios determined in our study are similar to those reported in 1995, 1998 and 1999 and partly overlap with years 1996, 2000 and 2001 (Monna et al., 1997; Noble et al., 2008) (Figure 2b). The $^{206}Pb/^{207}Pb$ determined for urban PM_{10} in our study fall within the range determined in France and the UK during mid-90s, that varied from 1.1008 to 1.1453 (Monna et al., 1997). Noble et al. showed that since leaded gasoline was banned in the UK in 1998, the $^{206}Pb/^{207}Pb$ ratio in urban PM in London shifted slightly from 1.1169-1.1388 to more radiogenic ratios during 2000 and 2001 and they stabilized thereafter (1.1354 - 1.1507). However, the road paint ($^{206}Pb/^{204}Pb$ = 17.866-18.301, $^{206}Pb/^{207}Pb$ = 1.1471-1.1708, $^{208}Pb/^{206}Pb$ = 2.0843-2.1012) and road dust ($^{206}Pb/^{204}Pb$ = 17.347-17.890, $^{206}Pb/^{207}Pb$ = 1.1163-1.1417, $^{208}Pb/^{206}Pb$ = 2.1176-2.1446) samples collected at the two sampling sites show significant Pb isotope ratio variability [redacted] illustrated in Figure 2a, the Pb isotope ratios of the PM fall on a mixing line with gasoline used in the UK before its phasing out as one end member (Monna et al. (1997) and road dust which contains re-mobilized Pb from leaded gasoline and other source deposits such as tires, brakes and road furniture as the other end member. The Pb isotope composition of the PM_{10} collected at NK and MR sites is similar to those of road dust and manhole cover which suggests that re-suspended road dust may contribute to Pb enrichment in urban PM. Previous elemental analyses of PM_{10} from the NK site showed appreciable concentrations of crustal elements such as Al and Ca, likely to have arisen from local soils (Beddows et al., 2015). Therefore, it seems likely that soils with residual contamination from the earlier use of leaded gasoline contribute to road dust which becomes resuspended into the atmosphere.

3.3 Copper and zinc isotope ratios variations in source materials and PM_{10}

The Cu and Zn isotope ratios of PM_{10} collected at the sites with high and low traffic densities and the potential local sources are illustrated in Figure 3. Previous published data for $PM_{2.5-80}$ collected in London between 2014 and 2015 and PM_{10} collected in Barcelona between 2012 and 2013 (Ochoa Gonzalez et al., 2016) are also shown for comparison. The $\delta^{65}Cu_{NIST976}$ values vary in the range between +0.01±0.13 ‰ and +0.51±0.10 ‰ at the MR site and between -0.01±0.10 ‰ and +0.46±0.07 ‰ at the NK site which indicates the same sources of Cu in the PM_{10} collected at the two sampling sites (Table S2-Sn). The $\delta^{66}Zn_{Lyon}$ values in PM collected at the MR site range between -0.14±0.04 ‰ and +0.33±0.04 ‰, and at the NK site between -0.21±0.14 ‰ and +0.26±0.12 ‰. Although high Cu and Zn concentrations are found at the high traffic site compared to the low traffic one (Table 1), the isotope data suggests that the dominant sources and/or controlling processes are the same at both sites. The similar variability in the Cu and Zn isotope ratios in the PM_{10} collected at the low and high traffic sites during 3 weeks over July 2010 (Figure 3) suggests that short-term temporal and spatial variations do not influence the sources of Cu and Zn in PM_{10} in London. This observation is in good agreement with previous studies that showed only significant isotope variability during the winter season between 2014 and 2015 and traffic sources being the main contributor to Cu and Zn enrichment in $PM_{2.5-80}$ in London (Ochoa Gonzalez et al., 2016). The Cu and Zn isotope ratios of $PM_{2.5-80}$ collected at building height during July and August 2014 and 2015 showed $\delta^{65}Cu_{NIST976}$ between +0.46±0.12 ‰ and +0.55±0.15 ‰ and $\delta^{66}Zn_{Lyon}$ between +0.02±0.04 ‰ and +0.17±0.02 ‰, with one light sample collected during summer 2015 ($\delta^{66}Zn_{Lyon}$= -0.29±0.04 ‰) (Ochoa Gonzalez et al., 2016). The Cu and Zn isotope signatures in PM_{10} collected in London at NK and MR sites in this study conducted during 2010 in London agree well with the isotope signatures in $PM_{2.5-80}$ collected in another street canyon during 2014 and 2015 in the same city (Ochoa Gonzalez et al., 2016).

293
294 *3.3.1. Sources of copper in urban particulate matter*
295 The sources (brakes, tires, manhole cover, road paint, road tarmac surface and road dust) have $\delta^{65}Cu_{NIST976}$
296 values ranging between -0.28±0.08 ‰ and +0.71±0.09 ‰ (Table S2-Sn). Four out of the six road dust samples
297 show copper isotope signatures within this range, with two samples showing negative isotope signatures
298 ($\delta^{65}Cu_{NBS976}$ = -0.28±0.08 ‰ and -0.07±0.09 ‰) at MR. Heavy Cu isotope signatures are found not only in
299 road paint, but also in road tarmac surface and specific samples of brakes and manhole cover which show
300 $\delta^{65}Cu_{NBS976}$ values above +0.55 ‰. The $\delta^{65}Cu_{NIST976}$ of the non-exhaust traffic sources (i.e., tires and brakes)
301 show a significant isotope variability, ranging between +0.17±0.10 ‰ and +0.33±0.12 ‰ for tires and between
302 +0.28±0.10 ‰ and +0.63±0.14 ‰ for brakes, most probably due to the different Cu species such as metallic Cu,
303 Cu oxides or Cu sulfides (Grigoratos and Martini, 2015; Straffelini et al., 2015) or possible isotopic
304 fractionation during the manufacturing processes.
305 Cu/Sb ratios in the PM have been used in several studies to identify source contribution of brake wear in
306 urban PM (Hjortenkrans et al., 2007b; Salma and Maenhaut, 2006; Weckwerth, 2001). The relationship
307 between the Cu/Sb ratios and the Cu isotope composition in the samples of PM analysed during this work and
308 previous studies conducted in Barcelona and London (Ochoa Gonzalez et al., 2016) are illustrated in Figure 4.
309 These results indicate that samples of PM_{10} from Barcelona and London with low Cu/Sb ratios between 5.8 and
310 11.6, which fall within the range of Cu/Sb found for brakes, show lighter Cu signatures with $\delta^{65}Cu_{NBS976}$
311 ranging between -0.01 and +0.51 ‰. Indeed, these isotope signatures largely overlap with the Cu isotope
312 signatures in samples of brakes analyzed during this study ($\delta^{65}Cu_{NIST976}$ = +0.28±10‰ - +0.63±14 ‰) (Table
313 S2-Sn). On the other hand, heavy Cu found in coarse particles ($PM_{2.5\text{-}80}$) in London ($\delta^{65}Cu_{NIST976}$ = +0.63
314 -+0.97 ‰) was attributed to combustion emissions which seemed more important during end-autumn and the
315 winter season (Ochoa Gonzalez et al., 2016).
316
317 *3.3.2. Sources of zinc in urban particulate matter*
318 The sources (brakes, tires, manhole cover, road paint, road tarmac surface and road dust) show $\delta^{66}Zn_{Lyon}$
319 ranging between -0.03±0.08 ‰ and +0.58±0.10 ‰ (Table S2-Sn). The Zn isotope signatures of the samples of
320 road dust range between +0.21±0.05 ‰ and +0.34±0.10 ‰ at both sites, except one sample with a $\delta^{66}Zn_{Lyon}$ of
321 -0.03±0.08‰ at the MR site, and they overlap with the signatures in PM_{10} at NK and MR sites. The variations
322 in the Zn isotope signatures found in the road dust samples at the two sites may reflect the potential
323 accumulation of different sources at the two locations. The Zn isotope signatures of the samples of manhole
324 cover, road paint and road surface are significantly different between samples from the same type with
325 differences up to 0.51 ‰ which suggests that the source materials and/or processes used during the
326 manufacturing of the various products may control the signatures. The heaviest Zn isotope signature has been
327 measured in road paint ($\delta^{66}Zn_{Lyon}$= +0.58±0.10 ‰). The Zn isotope composition of brakes and tires vary in a
328 small range with $\delta^{66}Zn_{Lyon}$ between +0.15±0.07 ‰ and +0.21±0.08 ‰ and are not significantly different
329 relative to an average internal precision of 0.08 ‰. According to this, we propose that Zn in PM_{10} at NK and
330 MR, that show $\delta^{66}Zn_{Lyon}$ ranging between -0.21 and +0.33 ‰, are derived from tires and brakes (Figure 3). The
331 Zn isotope composition are similar to the $PM_{2.5\text{-}80}$ collected at a high density traffic site in London during 2014
332 and 2015, with $\delta^{66}Zn_{Lyon}$ ranging between -0.29 and +0.17 ‰ (Figure 3). In addition, other sources enriched in

isotopically light Zn are missing to explain the light Zn found in three samples of PM_{10}, i.e., in NK3, MR8 and MR9 (Figure 3). We suggest that high temperature industrial emissions may be contributors to generate PM enriched in light Zn. Indeed, this is supported by the enrichment of V and Ni in the PM_{10} (Table 3), suggesting that high temperature industrial emissions may be relatively important. This hypothesis agrees with previous observations pointing that industrial processes such as smelting or combustion exert an effect on the fractionation due to evaporation and/or condensation processes (Mattielli 2009; Bigalke 2010; Ochoa Gonzalez 2015; Thapalia et al., 2015). The light Zn isotope signatures found in PM_{10} in Barcelona ($\delta^{66}Zn_{Lyon}$ = -0.83 ‰ to -0.45 ‰) were tentatively attributed to metallurgical emissions (Ochoa Gonzalez et al., 2016).

4. Conclusion

The aim of this study was to confirm the potential of stable metal isotopes (Cu, Zn and Pb) for tracing the sources of these metals in the urban atmospheric environment. Samples of PM_{10} and sources including road furniture (manhole cover, road paint and road tarmac surface), road dust and non-combustion sources (brakes and tires) were collected and analyzed for concentration and stable isotope ratios. Copper and Zn concentrations and EFs in the PM_{10} were higher at the high traffic site, along with other elements commonly associated with traffic related sources including Fe, Sb, Ba and Cr. In contrast, Pb showed no significant difference between the two sites although was enriched relative to crustal values.

The $^{206}Pb/^{207}Pb$ of PM_{10} ranges between 1.1137 and 1.1364, and the isotope ratios of Cu and Zn in the PM_{10} expressed as $\delta^{65}Cu_{NIST976}$ and $\delta^{66}Zn_{Lyon}$ range between -0.01 and +0.51 ‰ and between -0.21 and +0.33 ‰, respectively. No significant differences in the isotope signatures of these three metals between the two sites were found, suggesting similar sources at both sites. The stable isotope composition of Pb suggests that re-suspended road dust, which contains re-mobilized Pb from leaded gasoline, tires, brakes and road furniture, may dominate the emissions of Pb. The Cu and Zn signatures of tires, brakes and road dust overlap with the signatures of PM_{10}. The correlation between the enrichment of Sb and other tracers of brakes such as Cu, Fe and Ba in PM_{10} support the previous hypothesis that Cu is predominantly derived from non-exhaust traffic emissions in urban environments. The relationship between the Cu/Sb ratios and the Cu isotope composition demonstrates that samples of PM_{10} with low Cu/Sb ratios between 5.8 and 11.6, which fall within the range of Cu/Sb found for brakes, show lighter Cu with $\delta^{65}Cu_{NBS976}$ ranging between -0.01 and +0.51 ‰ and these isotope signatures largely overlap with the Cu isotope signatures in brakes ($\delta^{65}Cu_{NIST976}$ = +0.28±0.10 ‰ - +0.63±0.14 ‰). The Zn isotope signatures in PM_{10} at NK and MR overlap with the signatures of tires and brakes. However, additional sources not considered in this study, such as those from high temperature industrial emissions that impart isotopically light Zn, need to be invoked to explain the light signatures found in 3 out of 18 samples. This hypothesis is supported by the enrichment of V and Ni in the PM_{10}.

This work supports preliminary research suggesting that stable metal isotopes are a novel and powerful technique for source assessment of Cu, Zn and Pb in the environment. However, the results demonstrate that they do not allow distinguishing PM collected in sites with varying densities of traffic urban environments.

Acknowledgments

We thank Barry Coles and Katharina Kreissig for assistance in the MAGIC laboratories and Stanislav Strekopytov for the analysis by ICP-MS at the Natural History Museum. Johanna Gietl is thanked for her help

during sampling collection. Raquel Ochoa Gonzalez thanks the European Commission (FP7-PEOPLE-2012-IEF) for funding the project ISOTRACE (proposal 329878). We acknowledge financial support from the UK–China Scholarships for Excellence for Shuofei Dong.

References

Abdalmogith, S.S., Harrison, R.M., 2006. An analysis of spatial and temporal properties of daily sulfate, nitrate and chloride concentrations at UK urban and rural sites. J. Environ. Monit. 8, 691-699.

Adachi, K., Tainosho, Y., 2004. Characterization of heavy metal particles embedded in tire dust. Environment International 30, 1009-1017.

Beddows, D.C.S., Harrison, R.M., Green, D.C., Fuller, G.W., 2015. Receptor modelling of both particle composition and size distribution from a background site in London, UK. Atmos. Chem. Phys. 15, 10107-10125.

Bigi, A., Harrison, R.M., 2010. Analysis of the air pollution climate at a central urban background site. Atmospheric Environment 44, 2004-2012.

Brewer, G.J., 2010. Copper toxicity in the general population. Clin. Neurophysiol. 121, 459-460.

Cloquet, C., Carignan, J., Libourel, G., 2006. Isotopic composition of Zn and Pb atmospheric depositions in an urban/periurban area of northeastern France. Environmental Science & Technology 40, 6594-6600.

Cooper, J.A., Watson, J.G., 1980. Receptor Oriented Methods of Air Particulate Source Apportionment. Journal of the Air Pollution Control Association 30, 1116-1125.

Costa, D.L., Dreher, K.L., 1997. Bioavailable transition metals in particulate matter mediate cardiopulmonary injury in healthy and compromised animal models. Environ. Health Perspect. 105, 1053-1060.

Charron, A., Harrison, R.M., 2005. Fine (PM2.5) and coarse (PM2.5-10) particulate matter on a heavily trafficked London highway: Sources and processes. Environmental Science & Technology 39, 7768-7776.

Chen, J., Wang, W., Liu, H., Ren, L., 2012. Determination of road dust loadings and chemical characteristics using resuspension. Environ Monit Assess 184, 1693-1709.

Chen, L.C., Lippmann, M., 2009. Effects of Metals within Ambient Air Particulate Matter (PM) on Human Health. Inhalation Toxicology 21, 1-31.

Dong, S., Weiss, D.J., Strekopytov, S., Kreissig, K., Sun, Y., Baker, A.R., Formenti, P., 2013. Stable isotope ratio measurements of Cu and Zn in mineral dust (bulk and size fractions) from the Taklimakan Desert and the Sahel and in aerosols from the eastern tropical North Atlantic Ocean. Talanta 114, 103-109.

Flament, P., Mattielli, N., Aimoz, L., Choel, M., Deboudt, K., de Jong, J., Rimetz-Planchon, J., Weis, D., 2008. Iron isotopic fractionation in industrial emissions and urban aerosols. Chemosphere 73, 1793-1798.

Gamble, J.F., Lewis, R.J., 1996. Health and respirable particulate (PM(10)) air pollution: A causal or statistical association? Environ. Health Perspect. 104, 838-850.

Garg, B.D., Cadle, S.H., Mulawa, P.A., Groblicki, P.J., Laroo, C., Parr, G.A., 2000. Brake wear particulate matter emissions. Environmental Science & Technology 34, 4463-4469.

Geagea, M.L., Stille, P., Gauthier-Lafaye, F., Millet, M., 2008. Tracing of industrial aerosol sources in an urban environment using Pb, Sr, and Nd isotopes. Environmental Science & Technology 42, 692-698.

Gietl, J.K., Klemm, O., 2009. Analysis of Traffic and Meteorology on Airborne Particulate Matter in Münster, Northwest Germany. Journal of the Air & Waste Management Association 59, 809-818.

Gietl, J.K., Lawrence, R., Thorpe, A.J., Harrison, R.M., 2010. Identification of brake wear particles and derivation of a quantitative tracer for brake dust at a major road. Atmospheric Environment 44, 141-146.

Gioia, S., Weiss, D., Coles, B., Arnold, T., Babinski, M., 2008. Accurate and Precise Zinc Isotope Ratio Measurements in Urban Aerosols. Analytical Chemistry 80, 9776-9780.

417 Grigoratos, T., Martini, G., 2015. Brake wear particle emissions: a review. Environ Sci Pollut Res 22,
418 2491-2504.
419 Harrison, R.M., Deacon, A.R., Jones, M.R., Appleby, R.S., 1997. Sources and processes affecting
420 concentrations of PM10 and PM2.5 particulate matter in Birmingham (UK). Atmos Environ 31, 4103-4117.
421 Hjortenkrans, D.S.T., Bergbäck, B.G., Häggerud, A.V., 2007a. Metal Emissions from Brake Linings and Tires:
422 Case Studies of Stockholm, Sweden 1995/1998 and 2005. Environmental science & technology 41, 5224-5230.
423 Hjortenkrans, D.S.T., Bergbäck, B.G., Häggerud, A.V., 2007b. Metal emissions from brake linings and tires:
424 case studies of Stockholm, Sweden, 1995/1998 and 2005. Environ. Sci. Technol. 41, 5224-5230.
425 Hüner, R., Melcher, B., Milczarek, R., Kienleitner, H., 2001. Solid lubricants with a tin sulphide and carbon
426 base. Google Patents.
427 Iijima, A., Sato, K., Yano, K., Tago, H., Kato, M., Kimura, H., Furuta, N., 2007. Particle size and composition
428 distribution analysis of automotive brake abrasion dusts for the evaluation of antimony sources of airborne
429 particulate matter. Atmospheric Environment 41, 4908-4919.
430 Jarup, L., 2003. Hazards of heavy metal contamination. British Medical Bulletin 68, 167-182.
431 John, S.G., Park, J.G., Zhan, Z.T., Boyle, E.A., 2007. The isotopic composition of some common forms of
432 anthropogenic zinc. Chemical Geology 245, 61-69.
433 Laden, F., Neas, L.M., Dockery, D.W., Schwartz, J., 2000. Association of fine particulate matter from different
434 sources with daily mortality in six US cities. Environ. Health Perspect. 108, 941-947.
435 Lin, L., Lee, M.L., Eatough, D.J., 2010. Review of Recent Advances in Detection of Organic Markers in Fine
436 Particulate Matter and Their Use for Source Apportionment. J Air Waste Manage 60, 3-25.
437 Lough, G.C., Schauer, J.J., Park, J.S., Shafer, M.M., Deminter, J.T., Weinstein, J.P., 2005. Emissions of metals
438 associated with motor vehicle roadways. Environmental Science & Technology 39, 826-836.
439 Majestic, B.J., Anbar, A.D., Herckes, P., 2009. Stable Isotopes as a Tool to Apportion Atmospheric Iron.
440 Environmental Science & Technology 43, 4327-4333.
441 Manoli, E., Voutsa, D., Samara, C., 2002. Chemical characterization and source identification/apportionment of
442 fine and coarse air particles in Thessaloniki, Greece. Atmos Environ 36, 949-961.
443 Mattielli, N., Petit, J.C.J., Deboudt, K., Flament, P., Perdrix, E., Taillez, A., Rimetz-Planchon, J., Weis, D.,
444 2009. Zn isotope study of atmospheric emissions and dry depositions within a 5 km radius of a Pb-Zn refinery.
445 Atmos Environ 43, 1265-1272.
446 McKenzie, E.R., Money, J.E., Green, P.G., Young, T.M., 2009. Metals associated with stormwater-relevant
447 brake and tire samples. The Science of the total environment 407, 5855-5860.
448 Monna, F., Lancelot, J., Croudace, I.W., Cundy, A.B., Lewis, J.T., 1997. Pb isotopic composition of airborne
449 particulate material from France and the southern United Kingdom: implications for Pb pollution sources in
450 urban areas. Environ. Sci. Technol. 31, 2277-2286.
451 Moreno, T., Martins, V., Querol, X., Jones, T., BéruBé, K., Minguillón, M.C., Amato, F., Capdevila, M., de
452 Miguel, E., Centelles, S., Gibbons, W., 2015. A new look at inhalable metalliferous airborne particles on rail
453 subway platforms. Science of The Total Environment 505, 367-375.
454 Moreno, T., Perez, N., Querol, X., Amato, F., Alastuey, A., Bhatia, R., Spiro, B., Hanvey, M., Gibbons, W.,
455 2010. Physicochemical variations in atmospheric aerosols recorded at sea onboard the Atlantic-Mediterranean
456 2008 Scholar Ship cruise (Part II): Natural versus anthropogenic influences revealed by PM10 trace element

457 geochemistry. Atmos Environ 44, 2563-2576.
458 Noble, S.R., Horstwood, M.S.A., Davy, P., Pashley, V., Spiro, B., Smith, S., 2008. Evolving Pb isotope
459 signatures of London airborne particulate matter (PM10) - constraints from on-filter and solution-mode
460 MC-ICP-MS. J. Environ. Monit. 10, 830-836.
461 Nriagu, J.O., Pacyna, J.M., 1988. Quantitative assessment of worldwide contamination of air, water, and soils
462 by trace metals. Nature 333, 134-139.
463 Ochoa Gonzalez, R., Strekopytov, S., Amato, F., Querol, X., Reche, C., Weiss, D., 2016. New Insights from
464 Zinc and Copper Isotopic Compositions into the Sources of Atmospheric Particulate Matter from Two Major
465 European Cities. Environmental Science & Technology.
466 Ochoa González, R., Weiss, D.J., 2015. Zinc isotope variability in three coal-fired power plants: A predictive
467 model for determining isotopic fractionation during combustion. Environmental Science & Technology.
468 Ozkaynak, H., Xue, J., Spengler, J., Wallace, L., Pellizzari, E., Jenkins, P., 1996. Personal exposure to airborne
469 particles and metals: Results from the particle team study in Riverside, California. J Expo Anal Env Epid 6,
470 57-78.
471 Peltier, R.E., Lippmann, M., 2010. Residual oil combustion: 2. Distributions of airborne nickel and vanadium
472 within New York City. J Expo Sci Env Epid 20, 342-350.
473 Polissar, A.V., Hopke, P.K., Poirot, R.L., 2001. Atmospheric aerosol over Vermont: Chemical composition and
474 sources. Environmental Science & Technology 35, 4604-4621.
475 Prasad, A.S., Bao, B., Beck, F.W.J., Kucuk, O., Sarkar, F.H., 2004. Antioxidant effect of zinc in humans. Free
476 Radical Bio Med 37, 1182-1190.
477 Querol, X., Alastuey, A., Rodriguez, S., Plana, F., Ruiz, C.R., Cots, N., Massague, G., Puig, O., 2001. PM 10
478 and PM2.5 source apportionment in the Barcelona Metropolitan area, Catalonia, Spain. Atmos Environ 35,
479 6407-6419.
480 Rodriguez, S., Querol, X., Alastuey, A., Viana, M.M., Alarcon, M., Mantilla, E., Ruiz, C.R., 2004. Comparative
481 PM10-PM2.5 source contribution study at rural, urban and industrial sites during PM episodes in Eastern Spain.
482 Science of the Total Environment 328, 95-113.
483 Salma, I., Maenhaut, W., 2006. Changes in elemental composition and mass of atmospheric aerosol pollution
484 between 1996 and 2002 in a Central European city. Environmental Pollution 143, 479-488.
485 Samek, L., Stegowski, Z., Furman, L., 2016. Preliminary PM2.5 and PM10 fractions source apportionment
486 complemented by statistical accuracy determination, Nukleonika, p. 75.
487 Schauer, J.J., Rogge, W.F., Hildemann, L.M., Mazurek, M.A., Cass, G.R., Simoneit, B.R.T., 1996. Source
488 apportionment of airborne particulate matter using organic compounds as tracers. Atmos Environ 30,
489 3837-3855.
490 Sivry, Y., Riotte, J., Sonke, J.E., Audry, S., Schäfer, J., Viers, J., Blanc, G., Freydier, R., Dupré, B., 2008. Zn
491 isotopes as tracers of anthropogenic pollution from Zn-ore smelters The Riou Mort–Lot River system.
492 Chemical Geology 255, 295-304.
493 Straffelini, G., Ciudin, R., Ciotti, A., Gialanella, S., 2015. Present knowledge and perspectives on the role of
494 copper in brake materials and related environmental issues: A critical assessment. Environmental Pollution 207,
495 211-219.
496 Thorpe, A., Harrison, R.M., 2008. Sources and properties of non-exhaust particulate matter from road traffic: A

497 review. Science of the Total Environment 400, 270-282.
498 Thurston, G.D., Spengler, J.D., 1985. A quantitative assessment of source contributions to inhalable particulate
499 matter pollution in metropolitan Boston. Atmospheric Environment (1967) 19, 9-25.
500 Tong, S., von Schirnding, Y.E., Prapamontol, T., 2000. Environmental lead exposure: a public health problem
501 of global dimensions. B World Health Organ 78, 1068-1077.
502 Wåhlin, P., Berkowicz, R., Palmgren, F., 2006. Characterisation of traffic-generated particulate matter in
503 Copenhagen. Atmospheric Environment 40, 2151-2159.
504 Walsh, C.T., Sandstead, H.H., Prasad, A.S., Newberne, P.M., Fraker, P.J., 1994. Zinc: health effects and
505 research priorities for the 1990s. Environmental Health Perspectives 102, 5-46.
506 Weckwerth, G., 2001. Verification of traffic emitted aerosol components in the ambient air of Cologne
507 (Germany). Atmos Environ 35, 5525-5536.
508 Wedepohl, K.H., 1995. The composition of the continental crust. Geochim. Cosmochim. Acta 59, 1217-1232.
509 Weiss, D.J., Kober, B., Dalgopolova, A., Gallagher, K., Spiro, B., Le Roux, G., Mason, T.F.D., Kylander, M.,
510 Coles, B.J., 2004. Accurate and precise Pb isotope ratio measurements in environmental samples by
511 MC-ICP-MS. International Journal of Mass Spectrometry 232, 205-215.
512 Widory, D., Liu, X.D., Dong, S.P., 2010. Isotopes as tracers of sources of lead and strontium in aerosols (TSP
513 & PM2.5) in Beijing. Atmos Environ 44, 3679-3687.
514

515

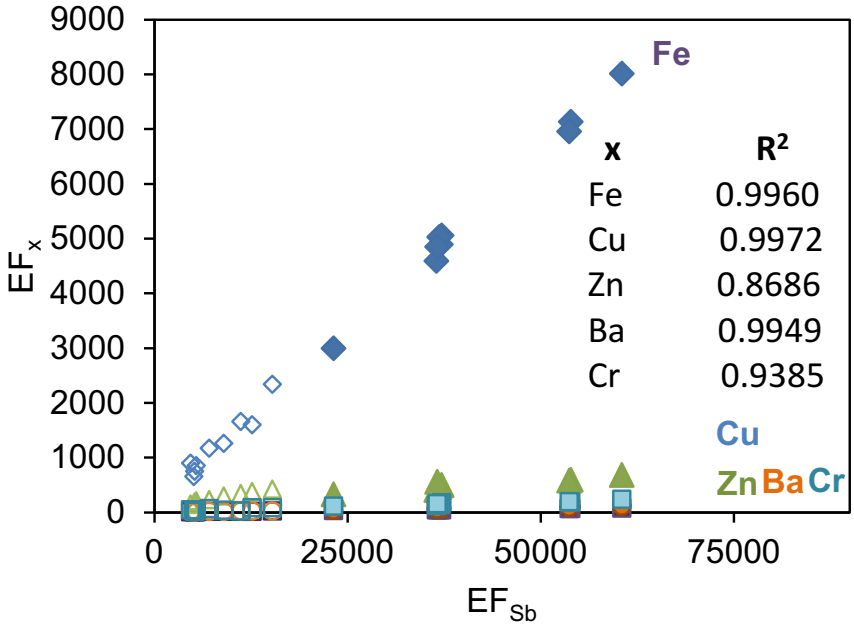


Figure 1. Relationship between the enrichment factors of Sb (EF_{Sb}) and the enrichment factors of X (EF_x) where x represents Fe, Cu, Zn, Ba and Cr in the PM_{10} collected in North Kensington (open symbols) and Marylebone Road (closed symbols).

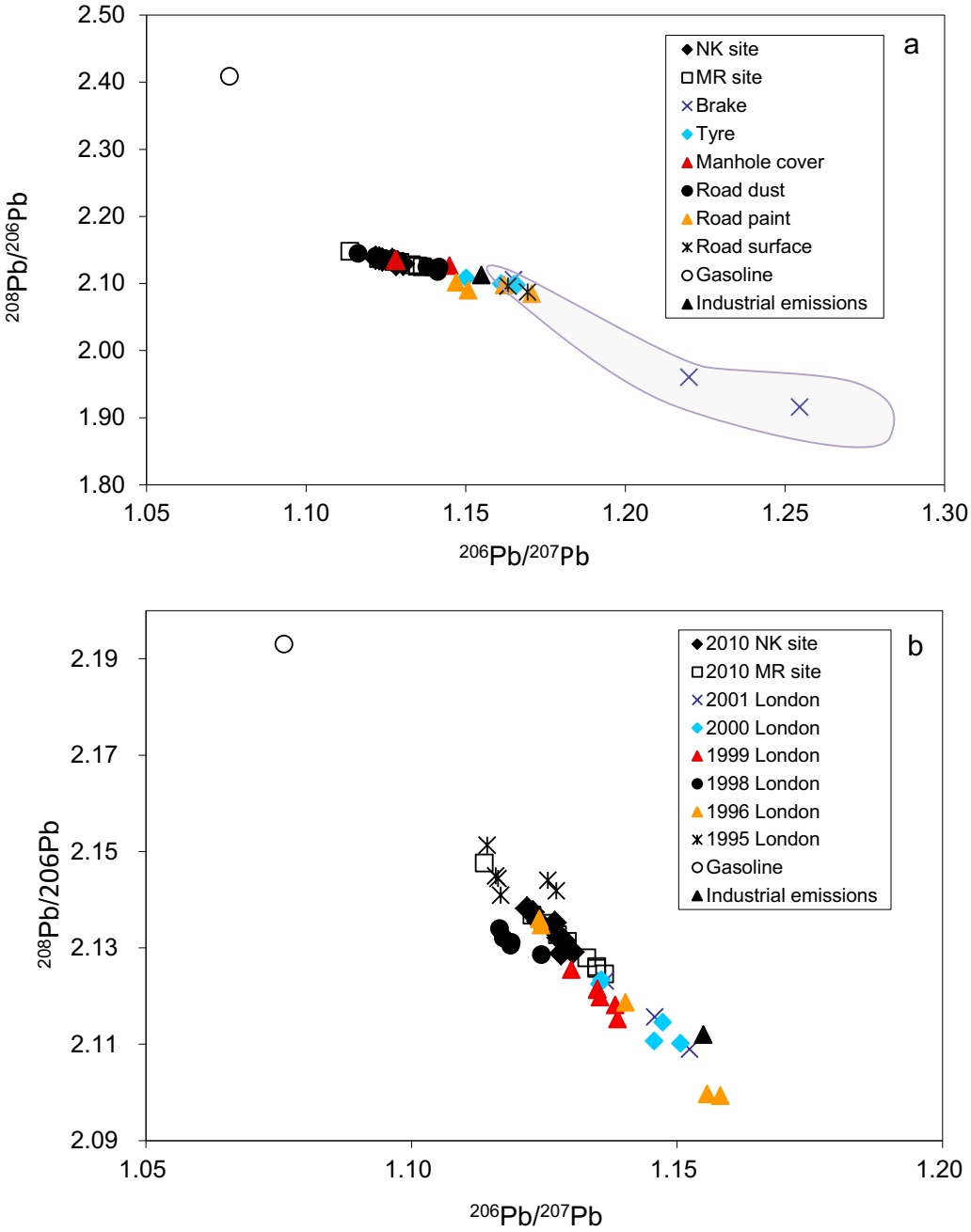


Figure 2. (a) $^{208}Pb/^{206}Pb$ versus $^{206}Pb/^{207}Pb$ plot of the PM_{10} samples collected in Marylebone (MR site) and North Kensington (NK site) and possible sources in this study; (b) $^{208}Pb/^{206}Pb$ versus $^{206}Pb/^{207}Pb$ plot of the PM_{10} measured in London since the phasing out of leaded gasoline between 1996 and 2001, as well as gasoline and industrial emissions (Noble et al. (2008) and Monna et al. (1997)) and during 2010 (this study). 2SD are not displayed in the figure as they are small and fall within the marker dimensions.

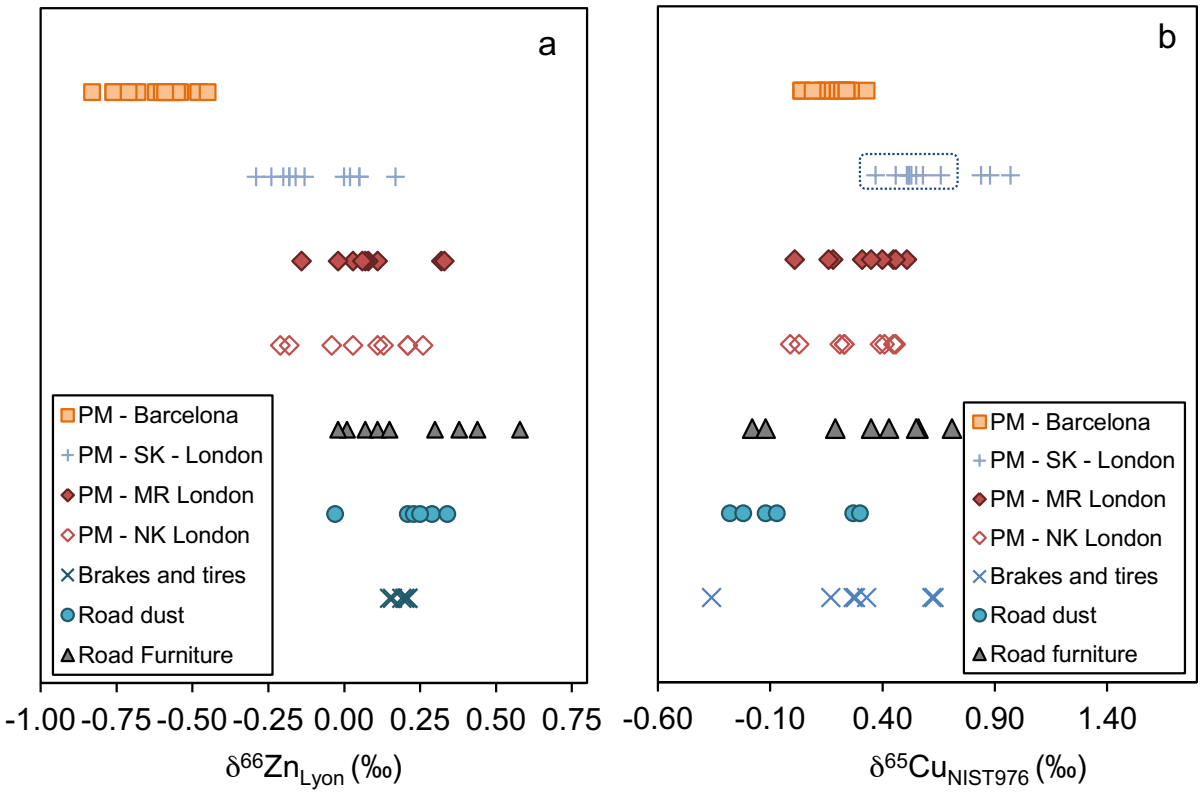


Figure 3. Zinc (a) and Cu (b) isotopic composition in PM_{10} collected at NK site (PM-NK London) and MR site (PM-MR London) and local sources during this study (summer 2010). Average 2SD for Zn and Cu isotope measurements are 0.08 and 0.10‰, respectively. Also shown are previous published isotope signatures in atmospheric $PM_{2.5-80}$ collected in London during 18 months between 2014 and 2015 and PM_{10} collected in Barcelona during two sampling campaigns in 2012 and 2013 (Ochoa Gonzalez et al., 2016) with average 2SD for Zn and Cu isotope ratios of 0.08 and 0.11‰, respectively.

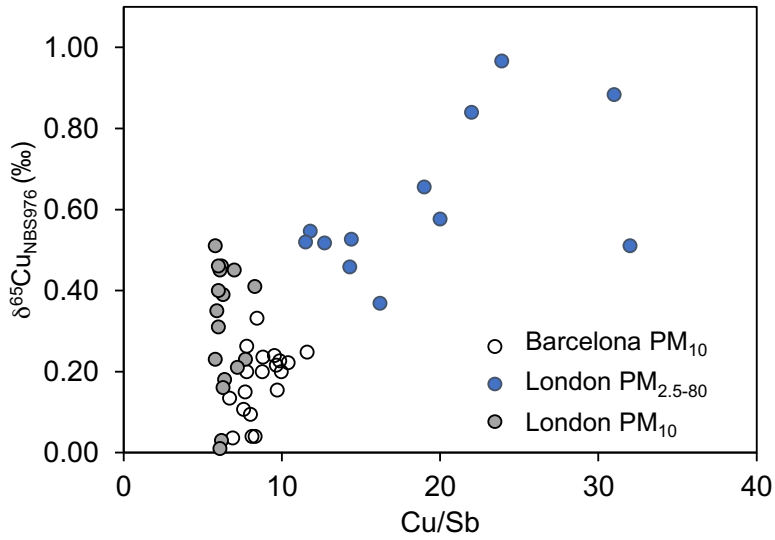


Figure 4. Relationship between Cu/Sb ratios and $\delta^{65}Cu_{NIST976}$ in PM_{10} collected at NK site and MR site in this study (London PM_{10}), and previous publish data in $PM_{2.5-80}$ from London (London $PM_{2.5-80}$) and in PM_{10} from Barcelona (Ochoa Gonzalez et al., 2016).

Table 1. Concentrations of PM_{10}, major and trace elements in the PM_{10} samples collected in Marylebone (MR) and North Kensington (NK), and Cu/Sb ratios.

Sample	Reference	Concentrations											Cu/Sb
		PM_{10} ($\mu g\ m^{-3}$)	Fe ($ng\ m^{-3}$)	Al ($ng\ m^{-3}$)	Cu ($ng\ m^{-3}$)	Zn ($ng\ m^{-3}$)	Sb ($ng\ m^{-3}$)	Ba ($ng\ m^{-3}$)	Pb ($ng\ m^{-3}$)	Cr ($ng\ m^{-3}$)	Ni ($ng\ m^{-3}$)	V ($ng\ m^{-3}$)	
NK - PM_{10}	NK1	12	78.6	22.8	3.1	2.9	0.5	2.0	1.3	0.2	0.5	0.7	6.2
	NK2	12	46.2	14.1	2.3	1.4	0.3	1.1	0.6	0.3	0.4	0.5	7.7
	NK3	10	66.0	13.4	3.1	2.7	0.5	1.7	1.3	0.2	0.2	0.3	6.2
	NK4	17	58.4	11.7	2.5	1.8	0.3	1.6	0.8	0.4	0.3	0.4	8.3
	NK5	15	46.2	6.1	1.9	1.4	0.3	1.2	0.7	0.1	0.2	0.2	6.3
	NK6	17	88.6	22.3	3.5	3.1	0.5	2.0	1.1	0.3	0.4	0.6	7.0
	NK7	15	68.0	8.2	3.6	2.3	0.5	1.9	0.9	0.3	0.2	0.2	7.2
	NK8	12	57.5	8.6	2.5	2.2	0.4	1.5	1.2	0.3	0.2	0.1	6.3
	NK9	14	86.9	28.6	3.5	2.8	0.6	1.8	1.4	0.4	0.2	0.1	5.8
	Average ± SD	14±2	66±16	15±8	2.9±0.6	2.3±0.6	0.4±0.1	1.6±0.3	1.0±0.3	0.3±0.1	0.3±0.1	0.3±0.2	6.8±0.9
MR - PM_{10}	MR1	37	2662.4	149.1	126.4	40.6	21.8	83.6	8.8	8.2	3.6	2.6	5.8
	MR2	28	550.2	20.0	26.4	8.0	4.3	17.6	1.1	1.7	0.7	0.6	6.1
	MR3	29	436.1	23.6	21.4	7.8	3.5	13.5	1.9	1.5	0.6	0.4	6.1
	MR4	38	481.2	25.2	23.5	8.4	3.7	14.9	1.4	1.9	0.9	0.4	6.4
	MR5	29	493.7	15.9	23.5	7.3	3.9	15.5	1.3	1.7	0.7	0.3	6.0
	MR6	41	640.9	35.3	32.8	10.6	5.2	20.1	1.8	2.5	1.0	0.8	6.3
	MR7	34	2301.2	89.3	114.7	34.8	19.2	71.5	6.8	7.8	2.7	1.5	6.0
	MR8	27	279.3	14.8	13.3	5.5	2.2	7.9	1.7	1.1	0.3	0.2	6.0
	MR9	18	211.9	17.0	9.4	3.7	1.6	5.7	1.2	0.9	0.3	0.1	5.9
	Average ± SD	31±7	-	-	-	-	-	-	-	-	-	-	6.1±0.2

Table 2. Concentrations of major and trace elements in local sources close to Marylebone (MR) and North Kensington (NK), including Cu/Sb ratios. '<' means below detection limit; '-' means not calculated.

Sample	Reference	Concentrations										Cu/Sb
		Fe ($mg\ g^{-1}$)	Al ($mg\ g^{-1}$)	Cu ($\mu g\ g^{-1}$)	Zn ($\mu g\ g^{-1}$)	Sb ($\mu g\ g^{-1}$)	Ba ($\mu g\ g^{-1}$)	Pb ($\mu g\ g^{-1}$)	Cr ($\mu g\ g^{-1}$)	Ni ($\mu g\ g^{-1}$)	V ($\mu g\ g^{-1}$)	
Brake	FSB-1	6.8	9.5	6.1	20.4	0.2	1018.0	5.3	89.2	50.6	9.7	27.3
	FSB-2	5.2	7.1	4.4	16.8	0.1	1288.4	4.0	79.7	40.9	7.0	39.3
	HBP-1	89.0	5.5	24.8	46.3	0.8	310.7	37.9	112.7	28.2	14.7	30.3
Tire	R43/54-1	0.4	0.2	42.8	8099.6	<	11.8	9.9	<	<	<	-
	R43/54-2	0.3	0.3	41.2	13273.9	<	18.5	13.6	<	1.4	<	-
	R56/57-1	0.2	0.4	26.4	7430.8	<	2.1	9.1	<	<	<	-
Manhole cover	NKMHC-1	67.9	5.7	52.0	371.0	7.4	552.9	693.0	129.9	103.2	25.8	7.0
	NKMHC-2	25.0	2.8	19.6	134.3	3.6	1055.1	56.4	93.2	86.3	15.4	5.4
	MRMHC-1	51.5	5.2	167.0	534.6	16.9	124.2	207.2	2317.6	1745.1	75.6	9.9
	MRMHC-2	43.0	1.5	89.3	417.3	7.5	115.2	88.8	123.5	110.0	115.3	11.9
Road dust	NKRD-1	9.4	4.4	70.1	217.0	3.3	93.2	138.2	28.8	11.0	19.0	21.2
	NKRD-2	7.6	3.2	17.0	80.1	1.0	33.9	22.4	28.5	100.5	14.9	17.0
	NKRD-3	18.2	12.9	24.8	165.1	0.7	86.3	25.5	30.5	17.8	56.0	35.4
	MRRD-1	16.7	6.0	801.4	556.4	20.9	163.8	409.8	55.3	26.0	23.2	38.3
	MRRD-2	14.1	3.7	74.2	349.3	10.1	96.5	168.7	53.7	12.7	15.0	7.3
	MRRD-3	10.0	4.0	140.2	353.3	39.5	93.6	54.3	39.7	16.8	14.4	3.5
Road paint	NKRP-1	0.6	0.3	1.8	43.9	<	2.4	2.8	3.2	4.0	0.5	-
	NKRP-2	0.4	0.2	<	4.8	93.1	196.3	3081.6	844.5	3.4	0.7	-
	MRRP-1	0.7	0.3	4.3	13.9	0.5	6.1	3.8	1.1	2.4	0.7	8.6
	MRRP-2	1.3	2.4	2.6	13.8	<	5.4	2.9	1.3	6.6	1.9	-
Road tarmac surface	NKRS-1	8.2	4.9	7.1	40.3	0.4	63.7	11.4	16.2	15.3	27.9	17.8
	NKRS-2	7.3	4.4	5.2	34.0	0.3	104.6	8.8	19.9	19.0	21.4	17.3

Table 3. Enrichment factors (EFs) in local sources and the PM_{10} samples collected at Marylebone (MR) and North Kensington (NK) sites. '-' means not calculated.

Sample	Reference	EFs								
		Fe	Cu	Zn	Sb	Ba	Pb	Cr	Ni	V
NK - PM_{10}	NK1	8.7	744.4	189.3	5254.1	10.1	258.0	17.9	82.7	43.9
	NK2	8.2	897.2	147.7	4730.8	9.0	198.8	47.0	111.7	53.8
	NK3	12.4	1257.3	298.6	9008.0	15.1	457.9	40.5	68.3	31.0
	NK4	12.6	1170.7	230.1	7132.5	16.1	316.9	67.0	102.7	44.7
	NK5	18.8	1657.0	342.9	11239.2	21.7	484.5	26.0	111.3	54.7
	NK6	10.0	847.3	208.6	5455.0	10.5	220.0	33.3	72.2	36.1
	NK7	20.7	2336.6	424.8	15278.4	26.7	483.8	81.0	94.7	37.3
	NK8	16.8	1593.8	376.9	12682.4	20.3	663.1	80.1	101.2	24.8
	NK9	7.6	653.2	144.6	5160.8	7.3	224.9	33.8	27.8	7.1
	Average±SD	13±5	1240±544	263±10	8438±3844	15±7	368±161	47±23	86±27	37±15
MR - PM_{10}	MR1	44.8	4592.7	405.2	36532.8	65.0	270.0	121.4	100.4	25.1
	MR2	68.9	7133.3	594.8	53920.7	101.9	245.3	187.5	150.7	44.0
	MR3	46.3	4896.1	489.1	37109.3	66.4	361.5	142.0	104.9	21.7
	MR4	48.0	5058.8	497.5	37217.5	68.5	246.7	171.1	148.5	24.9
	MR5	77.8	8009.7	682.3	60509.1	112.9	366.1	239.1	175.7	30.9
	MR6	45.5	5028.0	449.3	36901.3	66.0	232.1	155.8	116.0	31.4
	MR7	64.6	6956.7	579.7	53702.5	92.7	348.1	192.4	125.8	24.5
	MR8	47.3	4852.1	557.7	36603.3	62.2	518.4	158.9	93.1	19.0
	MR9	31.3	2991.8	327.5	23222.0	38.8	334.0	114.8	63.9	12.8
	Average±SD	53±15	5502±1557	509±10	41747±11755	75±23	325±90	165±38	120±34	26±9
Brake	FSB-1	1.8	3.5	3.2	5.9	12.5	2.6	20.9	22.3	1.5
	FSB-2	1.9	3.3	3.5	3.9	21.1	2.6	24.9	24.0	1.4
	HBP-1	40.7	24.5	12.6	37.2	6.6	31.5	45.5	21.4	3.9
Tire	R43/54-1	4.6	1162.4	60445.3	-	6.9	225.5	-	-	-
	R43/54-2	2.6	782.5	69293.6	-	7.5	217.2	-	20.6	-
	R56/57-1	1.5	396.0	30661.5	-	0.7	114.3	-	-	-
Manhole cover	NKMHC-1	29.8	49.3	96.7	325.0	11.2	552.6	50.3	75.2	6.6
	NKMHC-2	22.5	38.0	71.7	322.7	43.9	92.1	74.0	128.8	8.1
	MRMHC-1	24.5	171.4	150.9	799.7	2.7	178.9	971.8	1376.9	20.9
	MRMHC-2	73.4	329.0	422.8	1270.2	9.1	275.1	185.9	311.5	114.6
Road dust	NKRD-1	5.3	85.4	72.7	187.9	2.4	141.6	14.3	10.3	6.3
	NKRD-2	6.0	28.8	37.3	78.8	1.2	31.9	19.7	130.9	6.8
	NKRD-3	3.6	10.4	19.1	14.3	0.8	9.0	5.2	5.8	6.4
	MRRD-1	7.0	728.6	139.1	874.5	3.2	313.4	20.5	18.2	5.7
	MRRD-2	9.5	107.5	139.2	675.3	3.0	205.7	31.8	14.1	5.9
	MRRD-3	6.3	189.8	131.5	2464.4	2.7	61.8	22.0	17.4	5.3
Road paint	NKRP-1	4.6	27.5	188.4	-	0.8	36.8	20.5	47.7	2.2
	NKRP-2	5.1	-	39.1	125928.8	123.3	76043.9	10121.5	76.1	5.4
	MRRP-1	7.0	88.3	79.5	451.4	2.7	66.7	9.6	38.5	3.9
	MRRP-2	1.4	5.8	8.5	-	0.3	5.5	1.2	11.3	1.1
Road tarmac	NKRS-1	4.2	7.9	12.3	22.0	1.5	10.7	7.3	13.0	8.3
surface	NKRS-2	4.2	6.4	11.6	17.5	2.8	9.2	10.1	18.1	7.1

Table 4. Lead isotope ratios of PM_{10} samples collected at Marylebone Road (MR) and North Kensington (NK) and sources analyzed during this study. Each sample has been measured 3 or 4 times to calculate the 2SD.

Sample	Sample ID	Pb isotope ratios					
		$^{206}Pb/^{204}Pb$	2SD	$^{206}Pb/^{207}Pb$	2SD	$^{208}Pb/^{206}Pb$	2SD
NK - PM_{10}	NK1	17.446	0.004	1.1218	0.0001	2.1382	0.0002
	NK2	17.552	0.003	1.1277	0.0001	2.1327	0.0002
	NK3	17.465	0.005	1.1229	0.0001	2.1374	0.0002
	NK4	17.537	0.002	1.1270	0.0001	2.1352	0.0001
	NK5	17.554	0.003	1.1277	0.0001	2.1321	0.0001
	NK7	17.569	0.004	1.1287	0.0001	2.1315	0.0001
	NK8	17.598	0.004	1.1304	0.0001	2.1291	0.0001
	NK9	17.487	0.004	1.1239	0.0001	2.1355	0.0001
	NK10	17.564	0.003	1.1282	0.0001	2.1288	0.0001
MR - PM_{10}	MR1	17.512	0.002	1.1256	0.0001	2.1351	0.0001
	MR2	17.643	0.005	1.1330	0.0001	2.1279	0.0001
	MR3	17.581	0.005	1.1294	0.0001	2.1313	0.0002
	MR4	17.677	0.003	1.1349	0.0001	2.1261	0.0001
	MR5	17.550	0.002	1.1275	0.0001	2.1327	0.0001
	MR6	17.678	0.002	1.1349	0.0001	2.1257	0.0002
	MR7	17.701	0.003	1.1364	0.0001	2.1246	0.0001
	MR8	17.463	0.001	1.1227	0.0001	2.1368	0.0002
	MR9	17.305	0.002	1.1137	0.0001	2.1476	0.0001
Brake	FSB-1	19.569	0.003	1.2200	0.0001	1.9598	0.0001
	FSB-2	20.199	0.002	1.2547	0.0001	1.9151	0.0001
	HBP-1	18.176	0.004	1.1651	0.0001	2.1052	0.0001
Tire	R30-1	17.937	0.003	1.1502	0.0001	2.1075	0.0002
	R43/54-1	18.190	0.002	1.1660	0.0001	2.0973	0.0001
	R43/54-2	18.181	0.002	1.1653	0.0001	2.0983	0.0001
	R56/57-1	18.138	0.002	1.1613	0.0001	2.0995	0.0002
Manhole cover	NKMHC-1	17.883	0.003	1.1450	0.0001	2.1262	0.0001
	NKMHC-2	17.547	0.004	1.1281	0.0001	2.1355	0.0002
	MRMHC-1	17.557	0.004	1.1284	0.0001	2.1332	0.0001
	MRMHC-2	17.550	0.002	1.1280	0.0001	2.1335	0.0002
Road dust	NKRD-1	17.438	0.002	1.1218	0.0001	2.1403	0.0001
	NKRD-2	17.762	0.001	1.1405	0.0001	2.1222	0.0002
	NKRD-3	17.728	0.002	1.1379	0.0001	2.1245	0.0001
	MRRD-1	17.890	0.003	1.1417	0.0001	2.1242	0.0001
	MRRD-2	17.777	0.002	1.1412	0.0001	2.1176	0.0002
	MRRD-3	17.347	0.002	1.1163	0.0001	2.1446	0.0001
Road paint	NKRP-1	17.930	0.002	1.1509	0.0001	2.0894	0.0001
	NKRP-2	18.301	0.002	1.1708	0.0001	2.0843	0.0001
	MRRP-1	17.866	0.001	1.1471	0.0001	2.1012	0.0001
	MRRP-2	18.135	0.001	1.1621	0.0001	2.0973	0.0002
Road tarmac surface	NKRS-1	18.148	0.001	1.1633	0.0001	2.0953	0.0001
	NKRS-2	18.252	0.001	1.1695	0.0001	2.0869	0.0001

Supplementary Material

Click here to download Supplementary Material: Supplementary material.pdf